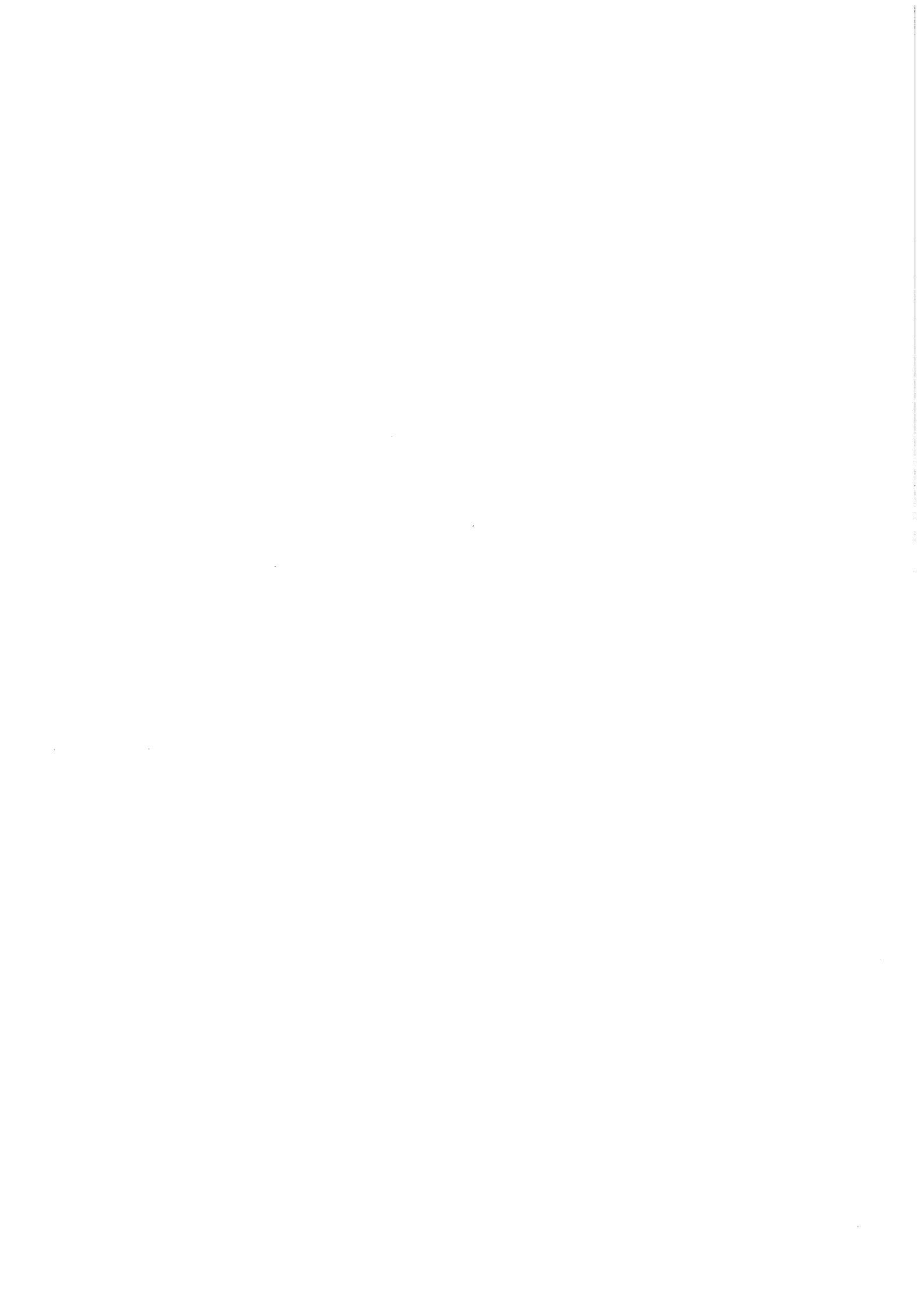


KfK 4573
Juni 1989

The Determination of the Dielectric Parameters of Ceramic Materials by Q-meter Measurements

R. Heidinger
Institut für Material- und Festkörperforschung
Projekt Kernfusion

Kernforschungszentrum Karlsruhe



KERNFORSCHUNGSZENTRUM KARLSRUHE
Institut für Material- und Festkörperforschung
Projekt Kernfusion

KfK 4573

**The determination of the dielectric parameters
of ceramic materials by Q-meter measurements**

R. Heidinger

Kernforschungszentrum Karlsruhe GmbH, Karlsruhe

Als Manuskript vervielfältigt
Für diesen Bericht behalten wir uns alle Rechte vor

Kernforschungszentrum Karlsruhe GmbH
Postfach 3640, 7500 Karlsruhe 1

ISSN 0303-4003

Abstract

A measuring facility based on a Q-meter system is described that provides the determination of the dielectric parameters of ceramics in the frequency range of 1 - 70 MHz. The dielectric parameters, the permittivity ϵ_r' and the loss tangent $\tan \delta$, are required for the selection of appropriate ceramic components in heating systems for nuclear fusion plasmas based on Ion-Cyclotron-Resonance Heating.

The theory of dielectric measurements by Q-meters is presented in detail. Further the basic formulae for the transformation of the measurable variables into ϵ_r' and $\tan \delta$ are developed for specimens with shapes of discs and rings. Their validity is checked for samples with diameters in the range of 30 - 50 mm and thicknesses in the range of 1 - 5 mm. A correction scheme is proposed for accounting for the influence of field distortion on the permittivity.

The influence of statistical and systematic errors are investigated, and it is found that the uncertainties introduced by the correction of field distortion dominate for ϵ_r' , whereas for $\tan \delta$ the statistical error is generally most important. The accuracy achieved for ϵ_r' is better than ± 0.3 , and the relative error of $\tan \delta$ amounts to $< 10\%$ for $\tan \delta$ values in the range of 10^{-3} - 10^{-4} .

Die Bestimmung der dielektrischen Parameter von keramischen Werkstoffen über Q-Meter-Messungen

Zusammenfassung

Es wird eine Meßeinrichtung auf der Grundlage eines Q-Meter-Systems beschrieben, die die Bestimmung der dielektrischen Parameter von Keramik im Frequenzbereich von 1 - 70 MHz erlaubt. Die dielektrischen Parameter, die Dielektrizitätskonstante ϵ_r' und der Verlusttanges $\tan \delta$, werden zur Auswahl geeigneter keramischer Komponenten in Heizsystemen für Kernfusionsplasmen, die auf der Ionen-Zyklotron-Resonanz beruhen, benötigt.

Die Theorie dielektrischer Messungen auf der Basis von Q-Metern wird im Detail dargelegt. Weiterhin werden die grundlegenden Formeln zur Umwandlung der Meßgrößen in ϵ_r' und $\tan \delta$ für scheiben- und ringförmigen Proben entwickelt. Ihre Gültigkeit wird für Proben mit Durchmessern im Bereich von 30 - 50 mm und mit Dicken im Bereich von 1 - 5 mm überprüft. Ein Korrekturschema wird vorgeschlagen, mit dem der Einfluß von Feldverzerrungen auf die Dielektrizitätskonstante berücksichtigt werden kann.

Der Einfluß statistischer und systematischer Fehler wird untersucht und es ergibt sich, daß die Ungenauigkeiten, die durch die Korrektur der Feldverzerrung eingeführt werden, für ϵ_r' überwiegen, währenddessen für $\tan \delta$ der statistische Fehler in der Regel am bedeutendsten ist. Eine Genauigkeit von besser als ± 0.3 wird für ϵ_r' erzielt und der relative Fehler in $\tan \delta$ liegt unter 10 % für Werte von $\tan \delta$ im Bereich von 10^{-3} - 10^{-4} .

Contents

1.	Introduction	1
2.	Dielectric measurements using a Q-meter set-up	2
2.1	Definition of the dielectric parameters	2
2.2	The principles of Q-meter measurements	2
2.3	Evaluation of Q-meter measurements	6
2.3.1	Disc-Shaped samples	6
2.3.1.2	Calculation of $\tan \delta$	9
2.3.1.3	Special cases	10
2.3.2	Ring-shaped Samples	11
2.4	The principles of the Q-factor measurements	13
2.4.1	Determination from the resonant amplitude	13
2.4.2	Determination from the resonance shape as a function of frequency	17
2.5	The procedure of dielectric measurements	19
2.5.1	Geometry of the samples	19
2.5.2	Determination of zero-error in measurement of electrode distance	21
2.5.3	The determination of the change ΔQ in the quality factor occurring when introducing the sample	21
2.5.4	The determination of the total capacitance C_T in the resonant circuit	22
3.	Discussion of experimental errors and correction techniques for extended sample sizes	23
3.1	Reproducibility of measurements	23
3.2	The correction for thin samples	24
3.3	The correction for samples with large diameter	27
3.4.2	Systematic errors in the permittivity measurements	31
3.4.3	Systematic errors in the dielectric loss measurements	32
4.	Dielectric parameters obtained for test materials	33
	References	36

1. Introduction

Radiofrequency heating is an important technique for raising and modeling the temperature profiles in nuclear fusion plasmas. In principle, three different frequency regimes are suitable, they are distinguished by the interaction which couples the electromagnetic waves to the ions of the plasma [1]. The Ion Cyclotron Resonance Heating (ICRH) at $10^7 - 10^8$ Hz and the Lower Hybrid Resonance Heating (LHRH) at about 10^9 Hz have already been tested in large Tokamak devices at the scale of long pulses and high power, while the Electron Cyclotron Resonance Heating (ECRH) at about 10^{11} Hz has so far been used at a much lower scale.

Ceramic components are needed as structural parts in the transmission lines for any of the different concepts. The research on dielectric properties of ceramics at KfK/IMF I, has laid a special interest to the frequency of ICRH in addition to the central concern in the microwave region for transmission windows in gyrotrons (power sources) to be used for ECRH [2]. A measuring equipment designed for the needs of the dielectric measurements in the MHz range, which is related to ICRH, was acquired from ERA, England*. It consists of an optimized commercial Q-meter (HP 4342 A), a sample head adapted to ceramic discs, and hardware and software components for registration and evaluation. It has already proved to be a sensitive tool to assign the deterioration of dielectric properties after fast neutron irradiation in polycrystalline and single crystal Al_2O_3 [3].

The equipment was originally designed for the disc-shaped specimens with a rather limited range of different size. Thus its performance had been specified and proved for discs with a diameter of 30 mm and thickness up to 2 mm. In practice it was found that the extension of its use to larger sizes was desirable, especially when short-termed investigations are performed that must necessarily work on samples with dimensions that are preferred by the supplier. In this context, discs with an inner hole, that will further on be called ring-shaped, will also be considered.

This report resumes in detail the fundamental physical relations which are involved with the use of Q-meters for dielectric measurements. The measurable variables are presented and basic relations are developed for their evaluation in terms of dielectric properties for disc- and ring-shaped samples. When these relations are applied to measurements on samples of different sizes, a systematic error on the dielectric constant appears due to fringing effects. A correction procedure is then proposed by which the systematic deviations can be reduced.

* ERA Technology Ltd, Cleve Road, Leatherhead, KT22 7SA, England

2. Dielectric measurements using a Q-meter set-up

2.1 Definition of the dielectric parameters

Dielectric properties, as discussed in this work, describe the influence of insulating materials on the propagation of electromagnetic waves. In a more general context, a full description of the material behaviour requires the knowledge of its complex dielectric constant ϵ_r^* and of its complex magnetic constant μ_r^* . But for all structural ceramics so far used in radiofrequency heating concepts, the magnetic behaviour can be well assigned by setting $\mu_r^* = 1$.

The complex dielectric constant is conventionally discussed in terms of the permittivity ϵ_r' ($= \text{Re } \epsilon_r^*$) and the dielectric loss tangent $\tan \delta$ ($= \text{Im } \epsilon_r^*/\text{Re } \epsilon_r^*$). In low loss dielectrics, it is only the permittivity that governs the reflection of the electromagnetic waves at material interfaces and the propagation speed in the bulk of the dielectric material through the impedance Z

$$Z = \sqrt{\frac{\mu_0}{\epsilon_0 \epsilon_r'}} \approx \frac{377}{\sqrt{\epsilon_r'}} \Omega. \quad [4]$$

The dielectric loss tangent combines with the permittivity to result in the dielectric loss factor that determines the absorbed power at a given field strength E_0 [5] (ω being the angular frequency $\omega = 2\pi f$):

$$P = \frac{\omega}{2} \epsilon_r' \tan \delta E_0^2.$$

In practice $\tan \delta$ varies over a much larger range for suitable dielectrics as ϵ_r' does. Therefore $\tan \delta$ is the key parameter for low absorption of electromagnetic power.

2.2 The principles of Q-factor measurements

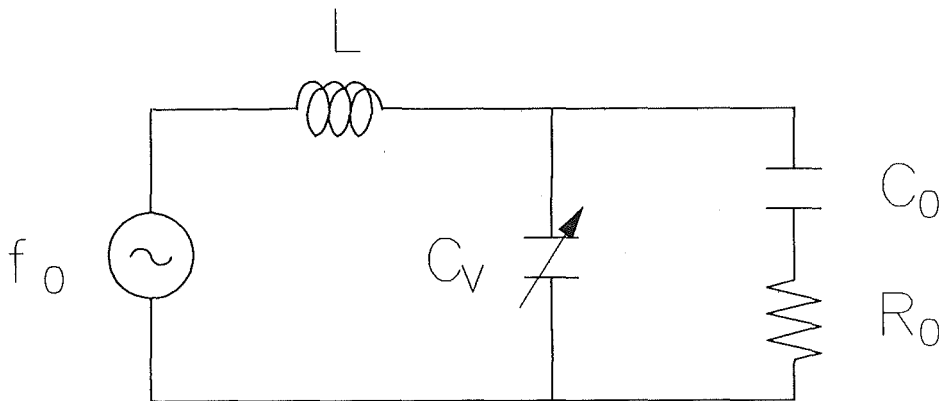
The dielectric material under investigation is introduced into a sample head and placed between a fixed and a movable electrode. The sample must be flat which particularly means that two lateral dimensions, which define the face part, must be comparable (max. 54 mm) and considerably larger than the third dimension (max. 5 mm), which defines the height. A demand for high measuring accuracy

implies an excellent machining of the sample dimensions, especially in the parallelism of the faces.

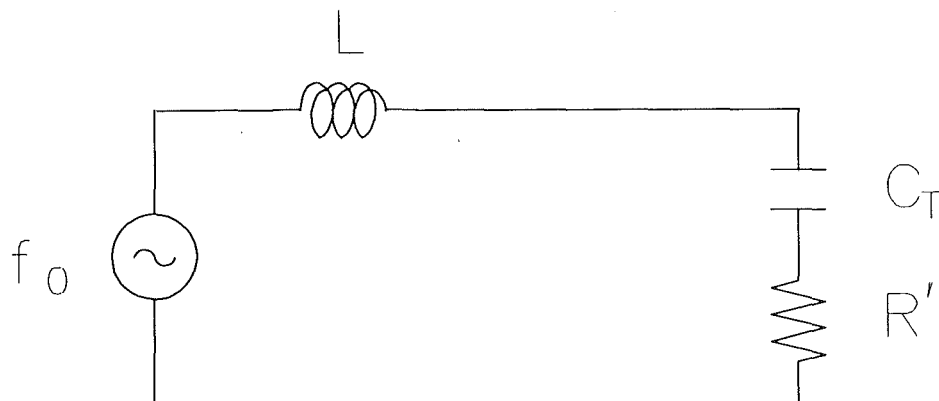
The experimental arrangement is identified as a capacitor with an inherent loss. The dissipation of energy in the capacitor can be described by a resistance R_0 in series to the non-dissipative capacitance C_0 . In this case the quality factor Q of the capacitor is defined by the relation:

$$Q = (\omega C_0 R_0)^{-1}$$

The Q-meter system determines Q for the capacitor in a resonant circuit brought to resonance at a selected frequency f_0 by adapting an inductive coil, L , and a variable capacitor C_v .



It is assumed that the dominant dissipative part in the circuit is caused by the sample head with the dielectric (R_0). The network is reduced to the following system for data analysis.



The transformation from R_0 to R' can be calculated by the complex impedance Z .

$$Z^{-1} = \left(\frac{1}{i\omega C_v} \right)^{-1} + \left(R_0 + \frac{1}{i\omega C_0} \right)^{-1}$$

$$Z^{-1} = \frac{-\omega^2 C_0 C_v R_0 + i\omega (C_0 + C_v)}{i\omega C_0 R_0 + 1}$$

$$Z = \frac{i\omega C_0 R_0 + 1}{-\omega^2 C_0 C_v R_0 + i\omega (C_0 + C_v)}$$

$$= \frac{\omega^2 C_0^2 R_0 + i\omega (\omega^2 C_0^2 R_0^2 C_v - (C_0 + C_v))}{\omega^4 C_0^2 C_v R_0^2 + \omega^2 (C_0 + C_v)^2}$$

For low dielectric loss, the dissipative part is small:

$$\omega^2 C_0^2 C_v R_0^2 \ll (C_0 + C_v)^2$$

and

$$\omega^2 C_0^2 C_v R_0^2 \ll C_0 + C_v$$

$$Z = \frac{\omega^2 C_0^2 R_0 - i\omega (C_0 + C_v)}{\omega^2 (C_0 + C_v)^2} = \frac{C_0^2}{(C_0 + C_v)^2} R_0 - \frac{i}{\omega (C_0 + C_v)}$$

$$Z = R' - \frac{i}{\omega C_T}$$

$$\Rightarrow C_T = C_0 + C_v \quad (2.1)$$

$$R' = \frac{C_0^2}{C_T^2} R_0 \quad (2.2)$$

If the dielectric absorption forms the only source of dissipation in the circuit, then an effective Q-factor can be defined for the circuit:

$$\frac{1}{Q_{\text{eff}}} = \omega C_T R' = \omega \frac{C_0^2}{C_T} R_0$$

The energy loss in the dielectric capacitor amounts to:

$$\omega C_0 R_0 = \frac{C_T}{C_0} \frac{1}{Q_{\text{eff}}} \quad (2.3)$$

When the dielectric is removed from the sample head, the resonant circuit will be detuned as the permittivity of the sample is not identical to the laboratory atmosphere. Quite generally, its permittivity is much higher and thus the electrodes of the sample head have to be approached until the same capacitance is attained and the resonance restored. The permittivity can be described by:

$$\epsilon_r = f(M_{\text{in}}, M_{\text{out}})$$

M_{in} : electrode distance with sample introduced

M_{out} : electrode distance without sample

The Q-factor of the resonant circuit without any sample introduced is clearly finite also, because of the residual dissipation caused in the components in the circuit. They have to be accounted for in evaluation of the measured Q-factors by introduction of second resistance R_r :

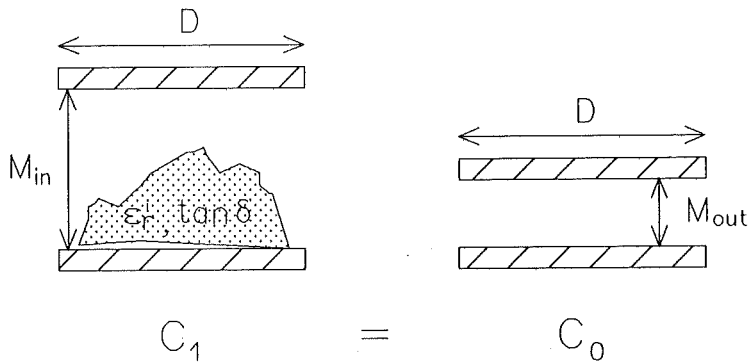
$$Q_{\text{in}} = \frac{1}{\omega C_T (R' + R_r)}$$

$$Q_{\text{out}} = \frac{1}{\omega C_T R_r}$$

$$\Rightarrow \frac{1}{Q_{\text{eff}}} = \frac{1}{Q_{\text{in}}} - \frac{1}{Q_{\text{out}}} \equiv \Delta \left(\frac{1}{Q} \right) \quad (2.4)$$

2.3 Evaluation of Q-meter measurements

Basically a capacitor formed by two disc-shaped electrodes of diameter D and an inserted dielectric sample is compared to a capacitor of the same capacitance formed by electrodes now at a smaller distance.

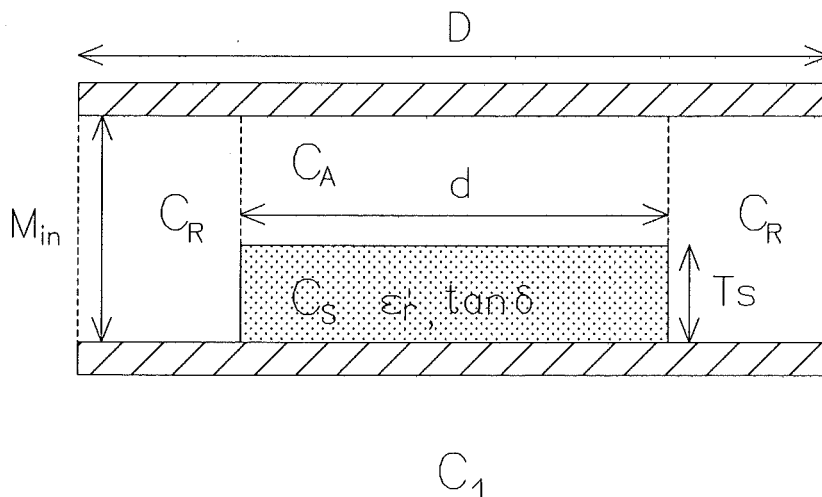


$$C_0 = \epsilon_0 \frac{D^2}{M_{out}} ; \epsilon_0 = \frac{\pi}{4} \epsilon_0 \quad (2.5)$$

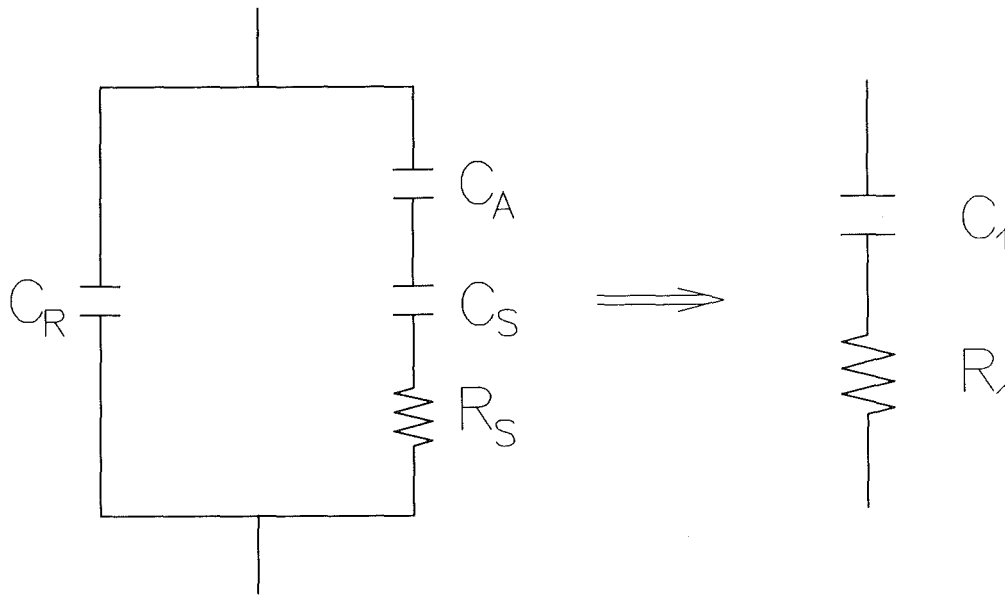
$$C_1 = f(\epsilon_r', M_{in}, D + \text{sample dimensions}) \quad (2.6)$$

As airgaps in the capacitor have to be admitted the permittivity of the sample is calculated from the contribution of the capacitance of the sample C_s to the capacitance of the whole capacitor C_0 . $\tan \delta$ first requires the calculation of the dilution of the dissipative part introduced by the dielectric in the ideally nondissipative air-filled parts of the capacitor ($R_s \Rightarrow R_0$). The calculations depend on the sample shape.

2.3.1 Disc-Shaped samples



Equivalent circuit:



$$C_i^{-1} = C_A^{-1} + C_S^{-1}$$

$$R_i = R_s \left(\frac{C_i}{C_i + C_R} \right)^2$$

Introduce first a normalized diameter f :

$$f = \begin{cases} \frac{d}{D} & \text{for } d < D \\ 1 & \text{for } d \geq D \end{cases} \quad (2.7)$$

$$C_R = \epsilon_0 D^2 \frac{1 - f^2}{M_{in}} \quad (2.8)$$

$$C_A = \epsilon_0 D^2 \frac{f^2}{M_{in} - T_s} \quad (2.9)$$

$$C_s = \epsilon_0 D^2 \epsilon_r' \frac{f^2}{T_s} \quad (2.10)$$

$$C_i = \epsilon_0 D^2 \epsilon_r' \frac{f^2}{T_s + \epsilon_r' (M_{in} - T_s)} \quad (2.11)$$

Reformulate the basic relation:

$$C_0 = C_1 = C_R + C_i$$

$$1 = \frac{C_R}{C_0} + \frac{C_i}{C_0}$$

$$1 = (1 - f^2) \frac{M_{out}}{M_{in}} + \frac{\epsilon_r' f^2 M_{out}}{T_s + \epsilon_r' (M_{in} - T_s)}$$

$$1 - \frac{(1 - f^2) M_{out}}{M_{in}} = \frac{f^2 M_{out}}{\frac{T_s}{\epsilon_r'} + (M_{in} - T_s)}$$

A normalized ratio is defined which describes the change in electric distance that is required to reset the capacitance after the removal of the dielectric:

$$D_K = 1 - (1 - f^2) \frac{M_{out}}{M_{in}} = \frac{C_0 - C_r}{C_0} \quad (2.12)$$

N.B. A useful relation between D_K and f^2 states:

$$f^2 \cdot M_{out} = D_K M_{in} + (M_{out} - M_{in}) \quad (2.13)$$

$$D_K = \frac{D_K M_{in} + (M_{out} - M_{in})}{\frac{T_s}{\epsilon_r'} + (M_{in} - T_s)}$$

$$\frac{T_s}{\epsilon_r'} + M_{in} - T_s = M_{in} + \frac{M_{out} - M_{in}}{D_K}$$

$$\frac{D_K T_s}{\epsilon_r'} = D_K T_s + M_{out} - M_{in}$$

$$\varepsilon_r' = \frac{D_K \cdot T_s}{D_K T_s + M_{out} - M_{in}}$$

where $D_K = 1 - (1 - f^2) \frac{M_{out}}{M_{in}}$

and $f = \begin{cases} \frac{d}{D} & \text{for } d < D \\ 1 & \text{for } d \geq D \end{cases}$

(2.14)

Note: If one replaces D_K and f by their formulation in terms d and D , one obtains

$$\varepsilon_r' = \frac{T_s [D^2 (M_{in} - M_{out}) + d^2 M_{out}]}{d^2 T_s M_{out} + D^2 (T_s - M_{in}) (M_{out} - M_{in})}$$

which is identical with the formulation of Barnett et al. [5].

2.3.1.2 Calculation of $\tan \delta$

The dielectric loss in the material is represented as a serial arrangement of a capacitance and a resistance. In this model $\tan \delta$ is calculated by:

$$\begin{aligned} \tan \delta &= \omega \cdot R_s \cdot C_s = \omega R_0 \frac{C_0^2}{C_i^2} C_s \\ &= \frac{C_T}{C_0} \frac{C_0 C_s}{C_i^2} \Delta (1/Q) \end{aligned}$$

formulae (2.3), (2.4) being applied.

The factor $C_0 C_s / C_i^2$ is evaluated on the basis of (2.5), (2.10), (2.11):

$$\frac{C_0 C_s}{C_i^2} = \frac{1}{M_{out}} \cdot \frac{\varepsilon_r' f^2}{T_s} \cdot \frac{\left(T_s + \varepsilon_r (M_{in} - T_s) \right)^2}{\varepsilon_r'^2 f^4}$$

$$= \frac{1}{f^2 M_{out}} \cdot \frac{1}{\varepsilon_r' T_s} \left(T_s + \varepsilon_r (M_{in} - T_s) \right)^2$$

in agreement with the formulation of Barnett et al [6].

The relation can be expressed in terms analogous to the determination of ε_r' with (2.13) and (2.14):

$$\begin{aligned} \frac{C_0 C_s}{C_i} &= \frac{1}{D_K M_{in} + M_{out} - M_{in}} \cdot \frac{1}{T_s} \cdot \\ &\cdot \frac{D_K T_s + M_{out} - M_{in}}{D_K T_s} \cdot \left(T_s + \frac{D_K T_s (M_{in} - T_s)}{D_K T_s + M_{out} - M_{in}} \right)^2 \\ &= \frac{1}{D_K} \frac{D_K T_s + M_{out} - M_{in}}{D_K M_{in} + M_{out} - M_{in}} \left(\frac{D_K T_s + M_{out} - M_{in} + D_K M_{in} - D_K T_s}{D_K T_s + M_{out} - M_{in}} \right)^2 \\ &= \frac{1}{D_K} \frac{D_K M_{in} + M_{out} - M_{in}}{D_K T_s + M_{out} - M_{in}} \end{aligned}$$

$$\boxed{\tan \delta = \Delta \left(\frac{1}{Q} \right) \frac{C_T}{C_0} \frac{1}{D_K} \frac{D_K M_{in} + M_{out} - M_{in}}{D_K T_s + M_{out} - M_{in}}} \quad (2.15)$$

2.3.1.3 Special cases

- Very large samples: ($d > D$) $F = 1$, $D_K = 1$

$$\varepsilon_r = \frac{T_s}{T_s + M_{out} - M_{in}} \quad (2.16)$$

$$\tan \delta = \Delta \left(\frac{1}{Q} \right) \frac{C_T}{C_0} \frac{M_{out}}{T_s + M_{out} - M_{in}} \quad (2.17)$$

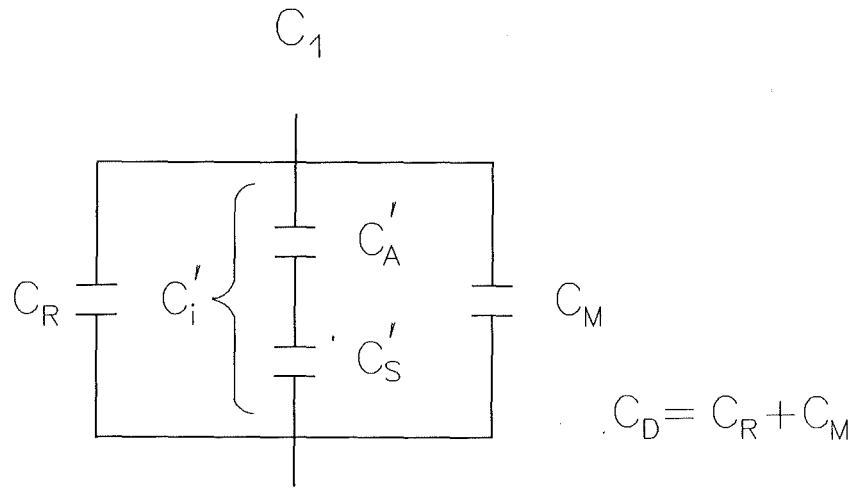
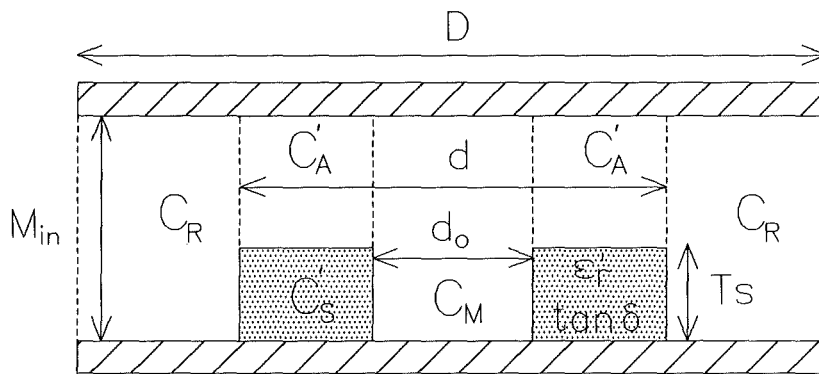
in agreement with the formulation of Pells et al. [6].

- No airgaps between sample and electrodes: $M_{in} = T_s$

$$\epsilon_r' = \frac{D_K T_s}{D_K T_s + M_{out} - T_s} = 1 + \frac{T_s - M_{out}}{f^2 M_{out}} \quad (2.18)$$

$$\tan \delta = \Delta \left(\frac{1}{Q} \right) \frac{C_T}{C_0} \frac{1}{D_K} \quad (2.19)$$

2.3.2 Ring-shaped Samples



$$C_R = \epsilon_0 \frac{D^2 - d^2}{M_{in}} \quad (2.20)$$

$$C_M = \epsilon_0 \frac{d_0^2}{M_{in}} \quad (2.21)$$

$$C_{A'} = \epsilon_0 \frac{d^2 - d_0^2}{M_{in} - T_s} \quad (2.22)$$

$$C_S' = \epsilon_0 \epsilon_r' \frac{d^2 - d_0^2}{T_s} \quad (2.23)$$

Normalized diameters are introduced

$$f = \begin{cases} \frac{d}{D} & \text{for } d < D \\ 1 & \text{for } d \geq D \end{cases}$$

$$g = \begin{cases} \frac{d_0}{D} & \text{for } d < D \\ 1 & \text{for } d \geq D \end{cases} \quad (2.24)$$

and $g < f$

$$C_D = C_R + C_M = \epsilon_0 D^2 \frac{1 - f^2 + g^2}{M_{in}} \quad (2.25)$$

$$C_i' = \left(C_{A'}^{-1} + C_{S'}^{-1} \right)^{-1} = \epsilon_0 D^2 \frac{\epsilon_r (f^2 - g^2)}{\epsilon_r (M_{in} - T_s) + T_s}$$

$$C_0 = C_1 = C_D + C_i'$$

$$1 = \frac{C_D}{C_0} + \frac{C_i'}{C_0}$$

$$1 = \frac{M_{out}}{M_{in}} (1 - f^2 + g^2) + M_{out} \frac{f^2 - g^2}{(M_{in} - T_s) + \frac{T_s}{\epsilon_r}}$$

The relation is equivalent to the relation for disc-shaped samples under the condition that f^2 is replaced by $f^2 - g^2$.

Therefore similar normalized ratios for electrode distances are introduced:

$$D_K = 1 - (1 - f^2) \frac{M_{out}}{M_{in}} \quad (2.26a)$$

$$D_g = -g^2 \frac{M_{out}}{M_{in}} \quad (2.26b)$$

$$D_{gK} = 1 - (1 - f^2 + g^2) \frac{M_{out}}{M_{in}} \quad (2.26c)$$

The determination of ϵ_r' corresponds to (2.14), with D_K now replaced by $D_{gK} = D_K + D_g$. The same reasoning is valid for the determination of $\tan \delta$. Therefore the following formulae are to be applied:

$$\epsilon_r' = \frac{D_{gK} \cdot T_s}{D_{gK} T_s + M_{out} - M_{in}}$$

$$\tan \delta = \Delta \left(\frac{1}{Q} \right) \frac{C_T}{C_0} \frac{1}{D_{gK}} \frac{D_{gK} M_{in} + M_{out} - M_{in}}{D_{gK} T_s + M_{out} - M_{in}} \quad (2.27)$$

with D_{gK} as defined by (2.24) and (2.26)

2.4 The principles of the Q-factor measurements

2.4.1 Determination from the resonant amplitude

The experimental determination of the Q-factor in the resonant circuit of the HP4342A has recourse on the basic properties of a forced oscillator with damping. The quality factor Q is defined by [4]:

$$Q = 2\pi \frac{\text{average energy stored per half cycle}}{\text{energy dissipated per half cycle}} \quad (2.28)$$

The differential equation describing the oscillator behaviour is common in many fields of physics and is generally discussed in the form [7]:

$$\ddot{x} + 2\delta \dot{x} + \omega_0^2 x = \frac{F_0}{m} e^{i\omega t} \quad (2.29)$$

It can be shown that the following relation holds for Q [8]:

$$Q = \frac{\omega^2 + \omega_0^2}{4\delta\omega} \quad (2.30)$$

The maximum amplitude A of the oscillator, i.e. the resonant amplitude, is a direct measure of Q, as can be seen as follows.

$$x = A \cos(\omega t + \phi) \quad (2.31)$$

$$A = \frac{F_0}{m} \left((\omega_0^2 - \omega^2)^2 + 4\delta^2 \omega^2 \right)^{-1/2} \quad (2.32)$$

$$= \frac{F_0}{m} \left((\omega_0^2 - \omega^2)^2 + \frac{(\omega^2 + \omega_0^2)^2}{4Q^2} \right)^{-1/2}$$

$$\frac{A m \omega_0^2}{F_0} = \left((1 - z)^2 + q(1 + z)^2 \right)^{-1/2} \quad (2.33)$$

with

$$z = \frac{\omega^2}{\omega_0^2}, \quad q = \frac{1}{4Q^2}$$

The maximum of a function of

$$f(g) = \frac{1}{\sqrt{g}}$$

equals to minimum of the function g.

$$g(z) = (1 - z)^2 + q(1 + z)^2$$

$$g'(z) = 2(z - 1) + 2q(z + 1)$$

$$g''(z) = 2 + 2q > 0$$

Because $g''(z) > 0$, the value of z that satisfies $g'(z) = 0$ is the value that gives the maximum of A:

$$z - 1 + q(z + 1) = 0$$

$$\Rightarrow (1 - z) = q(1 + z)$$

$$\text{and } z = \frac{1 - q}{1 + q}$$

$$\begin{aligned} A_{\max} &= \frac{F_0}{m \omega_0^2} \left(q^2(1 + z)^2 + q(1 + z)^2 \right)^{-1/2} \\ &= \frac{F_0}{m \omega_0^2} \frac{1}{(1 + z)} q^{-1/2} (q + 1)^{-1/2} \\ &= \frac{F_0}{m \omega_0^2} \frac{1}{2} (q + 1) q^{-1/2} (q + 1)^{-1/2} \\ &= \frac{F_0}{m \omega_0^2} \frac{1}{2} \sqrt{\frac{q + 1}{q}} = \frac{F}{m \omega_0^2} \sqrt{Q^2 + 1/4} \end{aligned}$$

because

$$\frac{1}{1 + z} = \frac{1 + q}{1 + q + 1 - q}$$

and

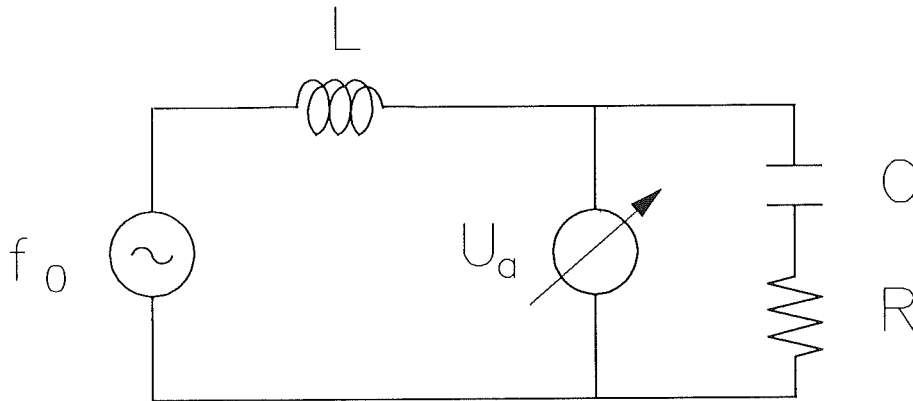
$$\frac{q + 1}{q} = 1 + 4Q^2$$

$$A_{\max} = \frac{F_0}{m \omega_0^2} \sqrt{Q^2 + 1/4} \quad (2.34)$$

The general problem is easily translated into the special case of a resonant circuit. As discussed in section 2.2 the dielectric material in the sample head acts as a serial arrangement of a capacitance and a resistance. It is set into a resonant circuit which further consists of a stable A.C. voltage source and of a suitable inductance L. The system can be described by [8]:

$$L \ddot{q} + R \dot{q} + \frac{q}{C} = U_0 e^{i\omega t} \quad (2.35)$$

where q is the electrical charge.



One measure the voltage between the low and high potential of the sample head:

$$U_a = \frac{q}{C} + R \dot{q} \approx \frac{q}{C} \quad (2.36)$$

$$\ddot{U}_a + \frac{R}{L} \dot{U}_a + \frac{1}{LC} U_a = \frac{1}{LC} U_0 e^{i\omega t} \quad (2.37)$$

Therefore the following correspondance is to be used in formula (2.34):

$$\Lambda_{\max} \Leftrightarrow U_{a, \max}$$

$$\frac{F_0}{m} \Leftrightarrow \frac{1}{LC} U_0$$

$$\omega_0^2 \Leftrightarrow \frac{1}{LC}$$

$$U_{a, \max} = U_0 \sqrt{Q^2 + 1/4} \quad (2.38)$$

With low loss materials, which were implicitly assumed already in (2.36), the term $1/4$ can be neglected relative to Q which amounts to some hundreds.

$$\frac{U_{a, \max}}{U_0} = Q \quad (2.39)$$

Therefore, at a fixed level of the voltage supply, the voltage at the sample head is a direct measure of Q .

2.4.2 Determination from the resonance shape as a function of frequency

The frequency dependence of the power absorbed inside the resonant circuit can be used for an alternative determination of Q.

The absorbed power $P(\omega)$ in a forced oscillator with damping described by (2.29) and (2.31) obeys the relation [7]:

$$P(\omega) = \delta \cdot m \cdot A^2 \cdot \omega^2. \quad (2.40)$$

In (2.32) the amplitude A near resonance is approximated with

$$\omega_0^2 - \omega^2 = (\omega_0 + \omega)(\omega_0 - \omega) \approx 2 \omega_0 (\omega_0 - \omega)$$

and

$$4m^2 \delta^2 \omega^2 \approx 4m^2 \delta^2 \omega_0^2$$

to yield:

$$A = \frac{F_0}{2m \omega_0} \left((\omega_0 - \omega)^2 + \delta^2 \right)^{-1/2}. \quad (2.41)$$

By insertion into (2.40) one obtains the absorbed power:

$$\begin{aligned} P(\omega) &= \delta \cdot m \cdot \frac{F_0^2}{4m^2 \omega_0^2} \cdot \frac{1}{(\omega_0 - \omega)^2 + \delta^2} \cdot \omega^2 \\ &= \frac{F_0^2}{4m} \frac{\delta}{(\omega_0 - \omega)^2 + \delta^2} \frac{\omega^2}{\omega_0^2}. \end{aligned} \quad (2.42)$$

As $\omega^2 \approx \omega_0^2$ near resonance:

$$P(\omega) = \frac{F_0^2}{4m} \frac{\delta}{(\omega_0 - \omega)^2 + \delta^2} \quad (2.43)$$

which is the well-known Lorentzian lineshape of resonance curves.

On the grounds of this relation, the quality factor of the resonant circuit is measured by introducing a power attenuator with a calibrated reduction factor

R and by noting this effect on the digit of the Q-meter which in practice shows U_a . The attenuator is removed and the same effect on U_a is reproduced by tuning the frequency off resonance to the frequency points ω_1 and ω_2 .

That means:

$$P(\omega_{1,2}) = R \cdot P(\omega_0). \quad (2.44)$$

Evaluating this relation for $\omega_{1,2}$, one obtains:

$$R = \frac{(\omega_0 - \omega_{1,2})^2 + \delta^2}{\delta^2}$$

$$\Rightarrow \omega_{1,2} = \omega_0 \pm \delta \sqrt{R - 1}$$

$$\Delta\omega = 2\delta \sqrt{R - 1} \quad (2.45)$$

with

$$\Delta\omega = \omega_2 - \omega_1.$$

The formula relating ω with δ (2.30) reduces for frequencies close to resonance to

$$Q = \frac{\omega_0}{2\delta}. \quad (2.46)$$

Therefore Q can be measured from the frequency width $\Delta\omega$ for given power attenuation R:

$$Q = \frac{\omega_0}{\Delta\omega} \sqrt{R - 1}. \quad (2.47)$$

For $R = 2$, $\Delta\omega$ is called half-width of the resonance ($\Delta\omega_{1/2}$). In this special case, the relation reduces to the well-known form:

$$Q = \frac{\omega_0}{\Delta\omega_{1/2}}. \quad (2.48)$$

2.5 The procedure of dielectric measurements

In principle, the relations deduced in section 2.3, such as (2.14) and (2.15) for disc-shaped samples and (2.18) and (2.19) for ring-shaped samples are exploited to determine ϵ_r' and $\tan \delta$. The experimental set-up, configured by ERA Technology as shown in figure 1, is accessed via a personal computer. The original software supplied by ERA was reformulated into an evaluation programme based on the APLxPLUS language. The programme leads the user through measurement in a dialogue form. The experimental parameters that are taken during the experiment are discussed in the following subsection:

2.5.1 Geometry of the samples

The diameter and the height of disc-shaped samples are asked for during the measuring programme. These data have to be determined before any dielectric measurement is undertaken.

The diameter is usually measured by sliding calipers with a precision of ± 0.05 mm. The sample head allows the introduction of a maximum diameter of 55 mm. The sample height is determined by placing the samples on an end measuring block and the height is taken in the centre of the sample. The precision of this technique is about ± 0.003 mm. Then the spots of maximum and minimum height are looked for near the sample rim and noted. The larger their difference, the larger the systematic error caused the deviation from the ideally parallel disc shape. Highly resolved measurements of the dielectric loss tangent ($\tan \delta \leq 10^{-4}$) should only be undertaken with samples where the deviation from parallelism is smaller than 10 μm . Maximum sample height is 5 mm.

The software transforms the measured parameters into the dielectric properties strictly for disc-shaped samples only. The basic measurable variables can of course also be determined for any flat sample of arbitrary form. If its lateral dimensions are considerably larger than the electrodes ($\varnothing 37$ mm), then they are seen by electrode in the same way as disc-shaped samples. For ring-shaped samples, an evaluation software supplies the dielectric properties subsequently to the measurements, provided the inner diameter of the ring is known.

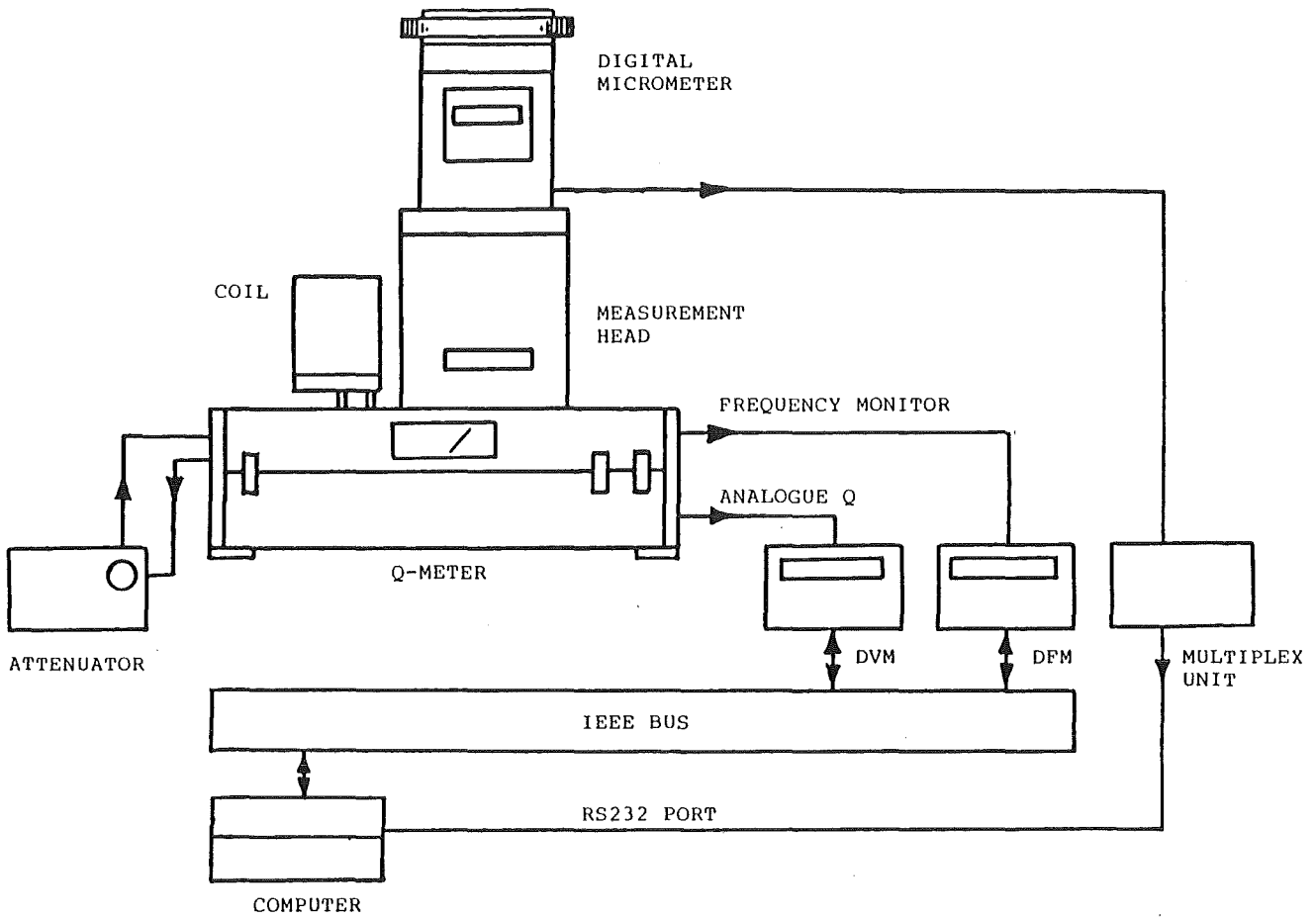


Fig. 1: Configuration of the Q-meter system.

2.5.2 Determination of zero-error in measurement of electrode distance

The electrode distance M_{in} and M_{out} is measured by a digital micrometer. Its zero point is arbitrary and usually set to the position in which the electrodes are in close contact. This choice must then be calibrated to absolute units by defining an zero error M_Z which is to be added to M_{in} and M_{out} :

$$M_{in} \rightarrow M_{in} + M_Z$$

$$M_{out} \rightarrow M_{out} + M_Z$$

The zero error is determined from the capacitance of the empty sample head at a given distance M :

$$C = C_s + C_v(M) = C_s + \frac{K}{M + M_Z}, \quad (2.49)$$

where C_s stray capacitance (25 pF)
 C_v variable capacitance
and K head constant (9.167 pF·mm).

A convenient test distance M is 200 μm .

2.5.3 The determination of the change ΔQ in the quality factor occurring when introducing the sample

The decrease $\Delta(1/Q)$ induced into the resonant circuit by the introduction of the sample is the most sensitive parameter in the measurement of the dielectric loss tangent. As one aims at the determination of a loss tangent of 5×10^{-5} with an equipment that has an inherent quality factor of 200 - 300, it is mandatory to choose the most reproducible determination of Q . This is realized by splitting up the determination of $\Delta(1/Q)$ into two steps.

$$\Delta(1/Q) = \frac{1}{Q_{in}} - \frac{1}{Q_{out}} = f(Q_{rel}) \cdot g(Q_{abs}),$$

with $f(Q_{rel}) = \frac{Q_{out} - Q_{in}}{Q_{in}}$

$$\text{and } g(Q_{\text{abs}}) = \frac{1}{Q_{\text{out}}} \quad (2.50)$$

For the term $f(Q_{\text{rel}})$, Q is only needed in relative units. The well resolved voltage U_a at resonance is therefore the best measure (c.f. subsection 2.3). It is generally connected with small zero error (Q_z) that is determined by setting the circuit into resonance when the sample is introduced and then detuning completely the resonance by removing the sample and setting the electrodes far apart. The value determined for U_a under these conditions is taken as a measure for Q_z and introduced into $f(Q_{\text{rel}})$:

$$f(Q_{\text{rel}}) \rightarrow \frac{Q_{\text{out}} - Q_{\text{in}}}{Q_{\text{in}} - Q_z} \quad (2.51)$$

For the term $g(Q_{\text{abs}})$, Q must be measured in absolute units. This requirement is better fulfilled by exploiting the Lorentzian form of the power stored in the circuit. The calibrated attenuator is compared to the frequency detuning that is needed to cause the same power reduction factor R (c.f. subsection 2.4):

$$g(Q_{\text{abs}}) = \frac{(\omega_2 - \omega_0) \sqrt{R - 1}}{\omega_0} \quad (2.52)$$

2.5.4 The determination of the total capacitance C_T in the resonant circuit

The dielectric loss tangent $\tan \delta$ (c.f. 2.15) is calculated using - besides the terms specific to dimensions of sample and the adjustments of the sample head - the term from the change in the quality factor and a third term consisting of the ratio between the total capacitance in the circuit C_T and the capacitance of the sample holder C_0 .

This term is called the dilution factor as it describes how the influence of the dielectric loss in the circuit is reduced by the additional capacitance present in the resonant circuit. The dilution factor is taken as C_T/C_S in the original software by Barnett et al. [5]. C_S is the capacitance contribution of the sample when the sample head is put into resonance with the sample introduced. It differs from C_0 by the neglect of the airgap term C_R and C_A which is a valid approximation in most practical cases.

3. Discussion of experimental errors and correction techniques for extended sample sizes

3.1 Reproducibility of measurements

The reproducibility of the measurements will be understood as the range of results obtained on the same type of materials and on a given sample shape. The reproducibility within a given measurement is generally estimated by repeating the experimental procedure at least three times and by taking the mean value and its standard deviation. In this work, the standard deviation is always indicated in brackets after the mean value and is given in units of the last figure of mean value.

The long term reproducibility that means reproducibility for measurements on the same sample performed after time intervals of some months, can be judged from Table 1. The data that were obtained for different discs of Al₂O₃ measured six months after the first measurements agreed within the standard deviations of the single measurement. The deviations in tan δ are in the order of 10 %. Great care was also taken that measurements could be performed in air with a relative humidity lower than 40 %.

Table 1: Long term reproducibility of dielectric measurements.
2 different AL995 discs from WESGO, Erlangen (30 mm dia, 1 mm thickness) measured at 9.4 MHz

Measured 9/87		Measured 3/88	
ϵ_r' a)	tan δ	ϵ_r' a)	tan δ
8.98 (11)	$7.0 (10) \cdot 10^{-5}$	9.01 (3)	$7.5 (1) \cdot 10^{-5}$
8.87 (13)	$8.1 (2) \cdot 10^{-5}$	9.02 (16)	$8.6 (2) \cdot 10^{-5}$

a) A correction term of + 0.6 must be added to obtain the absolute value of ϵ_r' (c.f. section 3.2)

If the reproducibility has to include measurements with samples of different sizes also, large discrepancies are encountered, as demonstrated in Table 2, especially for the permittivity. These discrepancies are caused by size effects that are not yet considered in the theory of data evaluation. Therefore the correction procedures described have to be applied.

Table 2: Dielectric measurements on samples with different size. Sintered AlN from Heraeus, Kleinostheim, measured at 1 MHz.

Sample size	ϵ_r'	$\tan \delta$
Ø 30 mm x 1 mm	8.09 (3)	$3.9 (1) \cdot 10^{-4}$
Ø 50 mm x 5 mm	11.80 (7)	$3.2 (1) \cdot 10^{-4}$

3.2 The correction for thin samples

Even when samples are used, that fulfill the standard shape for which the Q-meter is designed (i.e. 30 mm diameter), the measured permittivity has to be corrected by an empirical term for thin samples. This effect was described in the report of the acceptance test of the equipment and is due to the deviation from an homogeneous electrical field distribution which cannot be neglected for small samples.

A set of well-machined discs of optical glass (30 mm diameter, F2 glass, Schott, Mainz) was investigated to further quantify this effect. As can be seen in Table 3a the permittivity values increase with increasing sample thickness until they are kept constant for thickness larger than 3 mm. There is no such effect apparent in the values of dielectric loss tangent (c.f. Table 3b). Measurements on similarly well-machined set of AlN showed a similar increase in permittivity (c.f. Table 3c). On the base of these data, the correction terms listed in Table 4 were fixed that have to be added to the experimental results in order to be corrected for the limited thickness of the samples.

The more physical approach of avoiding this correction by including the distortion of the electrical field into the formulae of data evaluation requires more calibration data and the development of a more general description which has not yet been performed.

Table 3a: Permittivity as measured for a set of 30 mm discs out of F2 optical glass (Schott, Mainz).

Frequency	Sample height				
	1 mm	2 mm	3 mm	4 mm	5 mm
0.1 MHz	6.98 (7)	7.31 (2)	7.39 (1)	7.60 (1)	7.66 (4)
30 MHz	7.11 (5)	7.33 (4)	7.39 (2)	7.57 (3)	7.63 (4)
49 MHz	7.07 (7)	7.32 (1)	7.36 (2)	7.58 (2)	7.61 (1)
60 MHz	-	-	7.35 (2)	7.58 (2)	7.65 (2)
weighted mean value	7.07 (10)	7.32 (1)	7.38 (3)	7.59 (2)	7.62 (3)

Table 3b: Dielectric loss tangent as measured for the same sample set as in table 3a. Tan δ values in unit of 10^{-6} .

Frequency	Sample height				
	1 mm	2 mm	3 mm	4 mm	5 mm
0.1 MHz	482 (4)	485 (5)	490 (8)	496 (3)	494 (-)
30 MHz	850 (10)	860 (10)	860 (30)	870 (10)	870 (10)
49 MHz	1050 (20)	1050 (20)	1040 (10)	1010 (20)	1010 (30)
60 MHz	-	-	1010 (80)	1090 (30)	1050 (30)

Table 3c: Permittivity as measured for a set of 30 mm discs out of AlN (Tokuyama, Tokyo).

Frequency	Sample height		
	1 mm	1.4 mm	5 mm
7 MHz	8.09 (4)	8.17 (6)	–
10 MHz	8.10 (13)	8.20 (9)	–
25 MHz	8.16 (16)	8.17 (5)	8.82 (5)
30 MHz	7.90 (18)	8.07 (10)	8.79 (4)
47 MHz	–	8.10 (9)	8.72 (1)
50 MHz	–	8.17 (13)	–
weighted mean value	8.09 (9)	8.16 (7)	8.73 (4)

Table 4: Deviations in permittivity measurements as a function of thickness and assessment of the empirical correction term

	$\epsilon_r' (5 \text{ mm}) - \epsilon_r'$				
	1 mm	1.4 mm	2 mm	3 mm	4 mm
F2-glass	0.55	–	0.30	0.24	0.03
AlN	0.64	0.57	–	–	–
empirical correction term	0.6	0.5	0.3	0.2	0.0

3.3 The correction for samples with large diameter

The permittivity values obtained for samples with a diameter that is larger than the electrode diameter are apparently too high when calculated by the standard formulae (2.14) and (2.27). This is most easily demonstrated when samples of the same material with two different diameters, such as 30 mm and 50 mm, are compared (cf. Table 2).

The first approach to reconcile this disagreement was to vary the electrode diameter ($D = 37$ mm) in case that this parameter was not given correctly. But this variation affected the results for the samples of both diameters and proved to be rather insensitive. Allowing the limiting diameter, for which the sample still experiences the electrical field between the electrodes, to exceed the electrode diameter proved to be a key parameter. This can be understood by a sort of leaking out of the homogeneous electrical field into the sample outside the capacitor.

The procedure for correcting this effect was to redefine the normalized sample diameter f changing from its previous form (2.7) to:

$$f = \begin{cases} \frac{d}{D} & \text{for } d < f_{\max} \cdot D \\ f_{\max} & \text{for } d \geq f_{\max} \cdot D \end{cases} \quad (3.1)$$

with $f_{\max} \geq 1$

For f enters as f^2 into the formula (2.14) for calculating the permittivity, f_{\max}^2 and not f_{\max} was varied to remove the discrepancies in the measurements of 30 mm and 50 mm discs of SHAPAL-M and sintered AlN (cf. Table 5a, b). The best agreement was found with $f_{\max}^2 = 1.35$ in both cases. This value, however, was no suitable choice for the evaluation of the measurements performed on the 50 mm discs of KERSIT 301. The discs out of this material, which is a Si_3N_4 ceramic, were also measured at 30 - 40 GHz. There its permittivity amounted to 7.75. A general experience states that in low loss dielectrics the permittivity values do not differ much between the MHz and GHz range, and if there is a difference, the permittivity in the MHz range is slightly higher.

Table 5a: Dielectric data measured on SHAPAL-M, Tokuyama; evaluation with an extended range ($f^2_{\max} \geq 1$) in the values of the normalized sample diameter.

Sample size: \varnothing 50 mm, h = 5 mm, Frequency: 1 MHz

f^2_{\max}	1.0	1.05	1.10	1.15	1.20	1.25	1.30	1.35	1.40
ϵ_r'	9.76 (4)	9.32 (4)	8.91 (4)	8.55 (3)	8.21 (3)	7.91 (3)	7.62 (3)	7.37 (3)	7.13 (3)
$\tan \delta$ [10 ⁻⁴]	19.7 (1)	19.5 (1)	19.4 (1)	19.2 (1)	19.1 (1)	18.9 (1)	18.8 (1)	18.6 (1)	18.5 (1)

Note: Dielectric parameters measured on 30 mm sample:

$$\epsilon_r' = 7.3 \text{ (correction term for thin samples included)}$$

$$\tan \delta = 36 \cdot 10^{-4}$$

Table 5b: Dielectric data measured on sintered AlN, Heraeus; evaluation with an extended range ($f^2_{\max} \geq 1$) in the values of the normalized sample diameter.

Sample size: \varnothing 50 mm, h = 5 mm, Frequency: 1 MHz

f^2_{\max}	1.0	1.25	1.30	1.35	1.40
ϵ_r'	11.80 (7)	9.42 (4)	9.06 (3)	8.73 (3)	8.43 (2)
$\tan \delta$ [10 ⁻⁴]	3.2 (1)	3.0 (1)	3.0 (1)	3.0 (1)	2.9 (1)

Note: Dielectric parameters measured on 30 mm sample:

$$\epsilon_r' = 8.7 \text{ (correction term for thin samples included)}$$

$$\tan \delta = 3.9 \cdot 10^{-4}$$

Table 5c: Dielectric data measured on KERSIT301, Demarquest;
evaluation with an extended range ($f^2_{\max} \geq 1$) in the values of the
normalized sample diameter.

Sample size: \varnothing 44 mm x 4 mm, Frequency: 1 MHz

f^2_{\max}	1.0	1.05	1.10	1.15	1.20	1.25	1.35
ϵ_r'	8.28 (15)	7.90 (13)	7.55 (12)	7.24 (11)	6.96 (10)	6.70 (9)	6.24 (7)
$\tan \delta$ [10 ⁻⁴]	3.4 (1)	3.4 (1)	3.4 (1)	3.3 (1)	3.3 (1)	3.2 (1)	3.2 (2)

Empirical correction required for ϵ_r' : + 0.3

Table 5d: Dielectric data measured on Radiostea, Feldmühle
evaluation with an extended range ($f^2_{\max} \geq 1$) in the
values of the normalized sample diameter.

Sample size: \varnothing 50 mm x 2 mm, Frequency: 1 MHz

f^2_{\max}	1.0	1.05	1.10	1.15	1.20	1.25
ϵ_r'	7.72 (3)	7.32 (3)	6.96 (3)	6.65 (3)	6.36 (3)	6.10 (3)
$\tan \delta$ [10 ⁻⁴]	18.8 (1)	18.5 (4)	18.3 (4)	18.1 (4)	18.0 (4)	17.8 (4)

Empirical correction required for ϵ_r' : ± 0

Therefore one can use the permittivity value of the GHz range as a guideline. Upon examination of the results in Table 5c that are obtained for different values of f_{\max}^2 , one can conclude that a much smaller value than 1.35 must be chosen. The KERSIT 301 samples do not differ markedly from the SHAPAL-M and sintered AlN samples in regard of their dielectric parameters, they are, however, much thinner. Their sample height amounts to 2 mm instead of 5 mm. Therefore the suitable choice of f_{\max}^2 depends on sample thickness. Taking into account the empirical correction term that has to be added for thin samples, a value of $f_{\max}^2 = 1.10$ leads to a good result in permittivity. With the same considerations, it can be shown that $f_{\max}^2 = 1.20$ is a suitable choice for Radiostea discs (c.f. Table 5d), the permittivity of which should be close to 6.3 being a steatite material. Their sample height amounts to 5.0 mm, but they have a smaller diameter of 44 mm.

Resuming that the parameter f_{\max}^2 , which allows the extension of the electrode field into the sample beyond the electrode diameter, is a function of sample height and sample diameter, a tentative scheme can be set up for this dependence.

The electrode diameter is given to be 37 mm, therefore no extension into the sample will be expected for samples with a diameter of 35 mm and smaller. Also the extension disappears when the influence of sample is removed as the sample thickness tends to zero. Table 6 lists the scheme for f_{\max}^2 that has been obtained by interpolation between the three values fixed by experiment and the boundary conditions. Three more values of f_{\max}^2 have been taken out of this scheme to evaluate measurements with a diameter larger than 30 mm. The results are very satisfactory, especially when bearing in mind the strong changes introduced into the permittivity values by small changes of f_{\max}^2 .

Table 6: Empirical correction scheme for evaluating measurements on large discs. The electrical field is allowed to extend into the sample beyond the electrodes by setting $f_{\max}^2 \geq 1$. Values written in **bold** figures are fixed by experiment, values written in *italics* are used satisfactorily in evaluation.

Sample height [mm]	Sample diameter			
	35 mm	40 mm	45 mm	50 mm
0	1	1	1	1
1	1	1	1	1.05
2	1	<i>1</i>	1.05	1.1
3	1	1.05	1.10	1.2
4	1	<i>1.10</i>	1.15	1.25
5	1	1.10	1.20	1.35

3.4.2 Systematic errors in the permittivity measurements

The main sources of error in the determination of the permittivity are linked to the fringing of the electric field when the sample is thin and to an extension of the field when the sample is large. The fringing effect is small when the sample is thicker than 3 mm; it was shown in the acceptance test of the equipment that the permittivity of a 30 mm alumina sample determined with the present Q-meter corresponds within ± 0.2 to the value determined by a liquid immersion method, which is a totally independent technique. The fringing effect can be corrected by the empirical correction term for thinner samples and this term is fixed to at most 0.2 for neighbouring values of the sample height. Therefore the systematic error for samples with a diameter close to 30 mm can be taken as ± 0.2 .

For larger samples the extension of the electrical field has to be considered by setting $f_{\max}^2 \geq 1$ in (3.1). The empirical scheme of table 6 fixes f_{\max}^2 to ± 0.05 which means an error of ± 0.3 (c.f. Table 5) in the determination of the permittivity. For samples thinner than 4 mm, the error from the fringing of the electrical field has to be included, which leads to an error bar of about ± 0.4 .

In most cases, the systematic errors are larger than the error bars arising from the reproducibility. In the few other cases, where the reproducibility within a sample batch is of the same order, a range will be given for the permittivity.

3.4.3 Systematic errors in the dielectric loss measurements

The most sensitive factor in the determination of the dielectric loss tangent is the measurement of difference of the Q-factor when the sample is inserted and removed in the sample holder. As there is a time lag between two measurements in the order of some minutes, a systematic time trend of the voltage in the circuit will lead to systematic errors. It is found, however, that the instabilities are small and rather random in time. For a standard sized alumina sample (diameter 30 mm), it was proved that the dielectric loss tangent of two different Q-meter equipments with different sample holder correspond to 2×10^{-5} within an absolute value of 1×10^{-4} .

Fringing and field extension effects, that have be corrected for permittivity, are not as important for the dielectric tangent. The calibration with samples with different height out of F23 in table 3b show that there is no significant trend in the loss data and that the variation is of the order of 5 % at most. The permittivity correction for samples with large diameters via setting $f_{\max}^2 \geq 1$ induces an uncertainty in the dielectric loss tangent of < 10 %, but typically no more than 5 %.

Comparing the loss data for the samples of different sample size out of SHAPAL-M and sintered AlN (c.f. tables 5a, b) show larger discrepancy between the two sizes. Its reason is not quite clear, it may be related to intrinsic material behaviour.

Under the given conditions a systematic error of 10 % is believed to be justified, the uncertainty is increased in some cases by the reproducibility within a given batch of material.

4. Dielectric parameters obtained for test materials

The extension of the measuring technique aimed at adapting it to disc-shaped specimens with diameters up to 55 mm and thickness of 5 mm as well as to ring-shaped specimens. But in addition a data base of the dielectric parameters of the various test materials was determined. Besides the materials already mentioned in section 3, also a quartz glass, Hersail (Heraeus, Hanau), and a second alumina grade, AL300 (Wesgo, Erlangen) were investigated.

The dielectric properties are summarized in Table 6 and 7. Low loss dielectrics were measured with permittivities up to 10 and dielectric loss tangents ranging between $0.3 \cdot 10^{-5}$ and $2 \cdot 10^{-3}$. As the data base in literature is rather scarce, a direct comparison will not be performed at this stage. It is very reassuring, however, that the dielectric values stated for KER221 ceramics, such as steatite, in the international standard IEC 672-1 [9] were well found for the steatite supplied by Rauschert. The following values should be maintained for a KER221 ceramic: $\epsilon_r' = 6$ at 48 - 62 Hz and $\tan \delta \leq 12 \cdot 10^{-4}$ at 1 MHz.

Table 7a: Results of permittivity measurements on alternative ceramics.

Name and supplier of material	Main compounds	1 MHz	45 MHz	60 MHz
Steatite, Rauschert	MgO·SiO ₂	6.2 ± 0.3	6.2 ± 0.3	6.3 ± 0.3
SHAPAL-M, Tokuyama	AlN	7.3 ± 0.2	7.3 ± 0.2	–
AL300, Wesgo	Al ₂ O ₃	9.6 ± 0.2	9.6 ± 0.2	9.6 ± 0.2 ^b
AL995, Wesgo	Al ₂ O ₃	9.4 ± 0.2	9.5 ± 0.2	9.4 ± 0.2 ^b
KERSIT 301, Desmarquest	Si ₃ N ₄	7.9 ± 0.3	7.8 ± 0.3	7.8 ± 0.3
Sintered ALN, Heraeus	AlN	8.7 ± 0.2	8.7 ± 0.2 ^a	8.6 ± 0.2 ^c
F2-Glas, Schott	SiO ₂	7.7 ± 0.2 ^d	7.6 ± 0.2 ^e	7.7 ± 0.2
Herasil, Heraeus	SiO ₂	4.2 ± 0.2	4.2 ± 0.2	–
Translucent AlN, Tokuyama	AlN	–	8.7 ± 0.2 ^a	–

a Measured at 47 MHz

b Measured at 52 MHz

c Measured at 54 MHz

d Measured at 0.1 MHz

e Measured at 49 MHz

Table 7: Results of dielectric loss tangent measurements on alternative ceramics.

tan δ in units of 10^{-4}

Name and supplier of material	Main compounds	1 MHz	45 MHz	60 MHz
Steatite, Rauschert	MgO·SiO ₂	14 ± 1	17 ± 1	18 ± 1
SHAPAL-M, Tokuyama	AlN	20 ± 10	3 ± 1	–
AL300, Wesgo	Al ₂ O ₃	1.4 ± 0.1	2.3 ± 0.2	2.1 ± 0.4 ^b
AL995, Wesgo	Al ₂ O ₃	0.9 ± 1	0.8 ± 2	1.0 ± 1 ^b
KERSIT 301, Desmarquest	Si ₃ N ₄	3.4 ± 0.3	7 ± 1	7 ± 2
Sintered ALN, Heraeus	AlN	3.5 ± 0.5	0.7 ± 0.3 ^a	1.2 ± 0.2 ^c
F2-Glas, Schott	SiO ₂	4.8 ± 0.5 ^d	10 ± 1 ^e	10 ± 1
Herasil, Heraeus	SiO ₂	0.29 ± 0.05	0.33 ± 0.05	–
Translucent AlN, Tokuyama	AlN	–	1.0 ± 0.3 ^a	–

a Measured at 47 MHz

b Measured at 52 MHz

c Measured at 54 MHz

d Measured at 0.1 MHz

e Measured at 49 MHz

References

- [1] F. Leuterer
Heizung durch elektromagnetische Wellen
in J. Raeder et al., Kontrollierte Kernfusion, B.G. Teubner Stuttgart (1981)
130 - 160
- [2] R. Heidinger
Ceramic materials for microwave windows
Int. J. Electronics 64 (1) (1988) 37-48
- [3] R. Heidinger, F. Königer
Investigations on advanced ceramics for window applications in
radiofrequency heating concepts
J. Nucl. Mat. 155-157 (1988) 344-347
- [4] A. von Hippel
Dielectrics and Waves
The M.I.T. Press, Cambridge, Massachusetts (1966)
- [5] M. Barnett, G. Hill
Dielectric Test Set
Report on ERA Project 23-01-2850 (1987)
- [6] G.P. Pells, S.N. Buckley, G.J. Hill and M.J. Murphy,
Radiation effects in electrically insulating ceramics
Reporte AERE R 11715 (1985)
- [7] L.D. Landau, E.M. Lifschitz
Mechanik
Akademie Verlag Berlin (1963) 86-92
- [8] R.P. Feynman, R.B. Leighton, M. Sands
The Feynman Lectures on Physics, Vol. 1, Chapter 23, 24
Addison-Wesley, Reading, MA (1966)
- [9] Specifications for ceramic and glass insulating materials
IEC 672-1 (1980)